ChemistrySelect

Research Article
doi.org/10.1002/slct.202505556

Chemistry Europe
European Chemical Societies Publishing

www.chemistryselect.org

Anthracenyl-Hydrazinyl-Thiazolo Arene Ruthenium Complexes Coupled to Photosensitizers as PDT Agents

Chrysanthi Papadimou,[a] Frédérique Martin,[b] Bertrand Liagre,[b] and Bruno Therrien*[a]

Four anthracenyl-functionalized hydrazinyl-thiazolo pro-ligands (L_1-L_4) have been synthesized and characterized. Complexation to *p*-cymene ruthenium units has been conducted in methanol, affording four *p*-cymene ruthenium complexes [Ru(*p*-cymene)(η^2-**L**)Cl]Cl (abbreviated [**RuL$_{1-4}$**Cl]Cl). The ligands are coordinated to ruthenium by two nitrogen atoms, thus forming five-membered metalla-cycles. Then, these four arene ruthenium piano-stool complexes (**RuL$_{1-4}$**) were coordinated at the periphery of three pyridyl-functionalized porphyrin compounds, 5-pyridyl-10,15,20-triphenylporphyrin (**MPP**), 5,15-dipyridyl-10,20-diphenylporphyrin (**DPP**), and 5,10,15,20-tetrapyridylporphyrin (**TPP**), after removal of the chlorides in [**RuL$_{1-4}$**Cl]Cl by addition of silver triflate, to produce the corresponding dicationic [**MPP**(**RuL$_{1-4}$**)]$^{2+}$, tetracationic [**DPP**(**RuL$_{1-4}$**)$_2$]$^{4+}$ and octacationic complexes [**TPP**(**RuL$_{1-4}$**)$_4$]$^{8+}$. All organic molecules (L_1-L_4, **MPP**, **DPP**, **TPP**), organometallic complexes ([**RuL$_{1-4}$**Cl]Cl), as well as the 12 porphyrin arene ruthenium systems [**MPP**(**RuL$_{1-4}$**)](CF$_3$SO$_3$)$_2$, [**DPP**(**RuL$_{1-4}$**)$_2$](CF$_3$SO$_3$)$_4$ and [**TPP**(**RuL$_{1-4}$**)$_4$](CF$_3$SO$_3$)$_8$ have been tested as anticancer agents on the colon cancer cell line HCT116. In addition to cytotoxicity, the phototoxicity of the porphyrin-containing derivatives **MPP**(**RuL$_{1-4}$**), **DPP**(**RuL$_{1-4}$**)$_2$ and **TPP**(**RuL$_{1-4}$**)$_4$, together with **MPP**, **DPP**, **TPP,** and [**RuL$_{1-4}$**Cl]Cl, were evaluated under blue (420 nm, 20 J/cm^2), green (527 nm, 72 J/cm^2), and red (630 nm, 71 J/cm^2) light, showing a phototoxicity in the lower nanomolar range as well as excellent phototoxic indexes.

1. Introduction

The insertion of ruthenium (Ru) complexes in photodynamic therapy (PDT), in view to produce a synergetic effect between a photosensitizer (PS) and a Ru-based drug, has been studied for at least 30 years.[1,2] Ru-based drugs are promising chemotherapeutics,[3,4] as well as excellent antibacterial agents,[5] while the use of PS has seen a constant development since the commercialization of the first PDT agents.[6] Therefore, it is not surprising that the two modalities have been merged in single compounds and evaluated as photo-activating biological agents. Different strategies can be used to insert Ru in PDT modalities. Other that the coordination of a Ru(II) at the core of a first generation PS,[1,2] one consists of using the photochemical properties of polypyridyl–ruthenium complexes to be electronically involved in the photosensitizing process,[7–10] while another strategy consists of coordinating Ru-complexes at the periphery of a more traditional PS (porphyrin, phthalocyanine).[11–13] The second strategy limits the electronic impact on the photo-chemistry of the PS, but modify other properties such as solubility, lipophilicity, and bio-activity (Figure 1). Nevertheless, all strategies have been extensively explored in PDT.

Traditional PS tend to aggregate, as they are often porphyrin-based compounds.[14,15] Such planar aromatic derivatives possess a large conjugated surface, thus favoring $\pi-\pi$ stacking interactions in aqueous solution, which can often block the photochemical process to take place. Consequently, instead of functionalizing porphyrin-based compounds through organic chemistry transformations,[16] limiting aggregation can also be achieved by coordination chemistry.[11–13] Like organic groups, introduction of complexes at the periphery of PS reduces the $\pi-\pi$ stacking surface, adding knots that can be hydrophilic or charged, and offering the possibility to fine-tune the water solubility, bio-activity and bio-distribution of the PS, while limiting aggregation. Arene Ru-complexes are particularly appealing for this manner, being water soluble,[17] having several coordination sites, and quite easy to synthesize.[18] They are also biocompatible, with cytotoxicity being mostly associated to the nature of the ligands, not the metal.[19–22] Consequently, several arene Ru-complexes have been associated to PS and evaluated as anticancer agents.[23,24]

Among arene Ru-complexes, those with chelating ligands are particularly attractive to ensure coordination stability. Often, monodentate ligands are labile,[25] which can be advantageous or not, depending on the kinetics of the process, the nature of the ligands, or the exchanged mechanism involved. A rapid release, before reaching the target is counterproductive, however, after internalization, it might be beneficial to have the ligand being freed.[26] Nevertheless, chelating ligands are expected

[a] *Dr. C. Papadimou, Prof. B. Therrien*
Institute of Chemistry, University of Neuchatel, Avenue de Bellevaux 51, Neuchatel CH-2000, Switzerland
E-mail: bruno.therrien@unine.ch

[b] *F. Martin, Prof. B. Liagre*
LABCiS, UR 22722, Faculté de Pharmacie, Université de Limoges, Limoges F-87000, France

Supporting information for this article is available on the WWW under https://doi.org/10.1002/slct.202505556

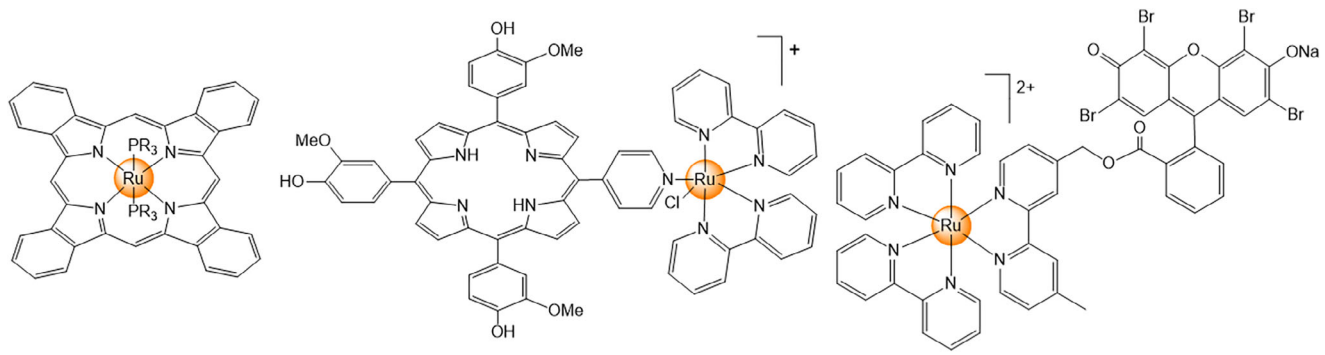

Figure 1. Selected examples of Ru-based PDT agents, with the ruthenium being at the core (left) of the PS,[1] at the periphery (center)[11] or electronically involved (right).[7]

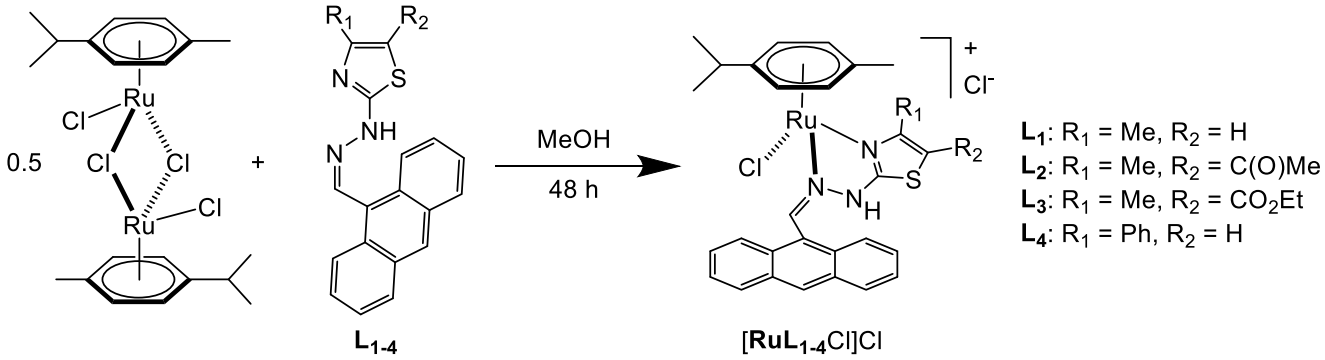

Scheme 1. Synthesis of the monocationic arene ruthenium complexes [Ru(*p*-cymene)(η^2-**L**)Cl]Cl ([**RuL$_{1-4}$**Cl]Cl) from **L$_1$**-**L$_4$** and [Ru(*p*-cymene)Cl$_2$]$_2$.

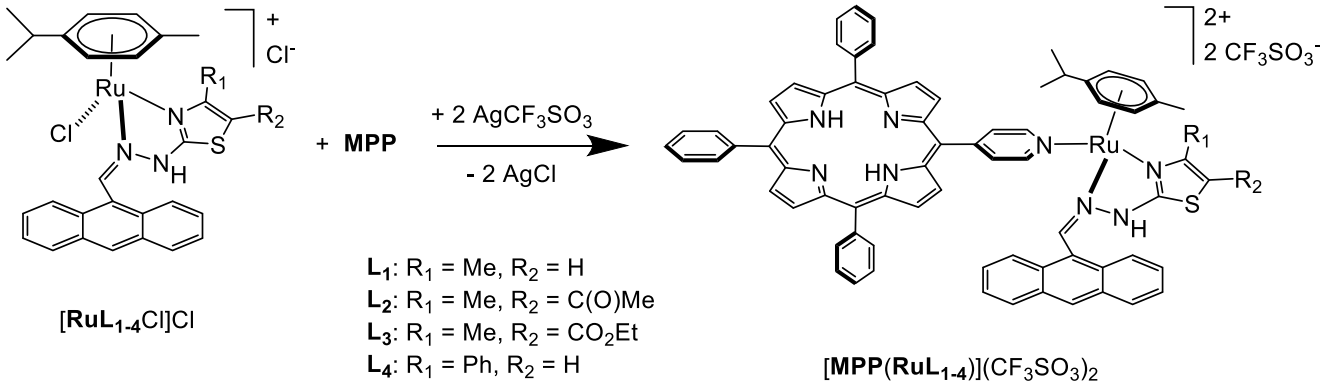

Scheme 2. Synthesis of the dicationic *p*-cymene Ru-porphyrin-based complexes [**MPP**(**RuL$_{1-4}$**)](CF$_3$SO$_3$)$_2$.

to stay attached to the Ru-center for longer periods, and enter cells together with the arene Ru-unit, thus forming a stable (arene)RuL entity (L = ligand). Hydrazinyl–thiazole derivatives are well-known pharmacophores,[27,28] and they are generally N∩N or N∩O double-coordinated to arene Ru-complexes.[29–31] Moreover, they are easy to synthesize,[32] and they can be functionalized in several positions, thus being ideal for drug design optimization, and accordingly, to be used as chelating ligands with arene Ru-complexes.

Colorectal cancer (CRC) remains one of the most deadliest cancer,[33] despite progress in prevention, early diagnosis and improved treatments.[34] The disease follows different pathways, involves various mechanisms, and therefore, demands multiple treatment modalities to increase survival rate.[35] PDT is an emerging option for treating CRC, and it offers great perspectives,[36] but it hasn't reach the clinic yet. Therefore, there is a tremendous interest in developing new PDT agents for CRC, especially in combination with other therapy. We have recently evaluated the potential of arene Ru–porphyrin derivatives on colon Colo205 cancer cells, and found that the arene Ru-units were crucial for the internalization of the PS and the biological activity.[23] Moreover, our results confirmed that production of reactive oxygen species (ROS) in the vicinity of the PS localization was responsible for cell death, and that the presence of arene-Ru units did not hamper the PDT efficiency. Therefore, based on these results and to potentially increase the amount

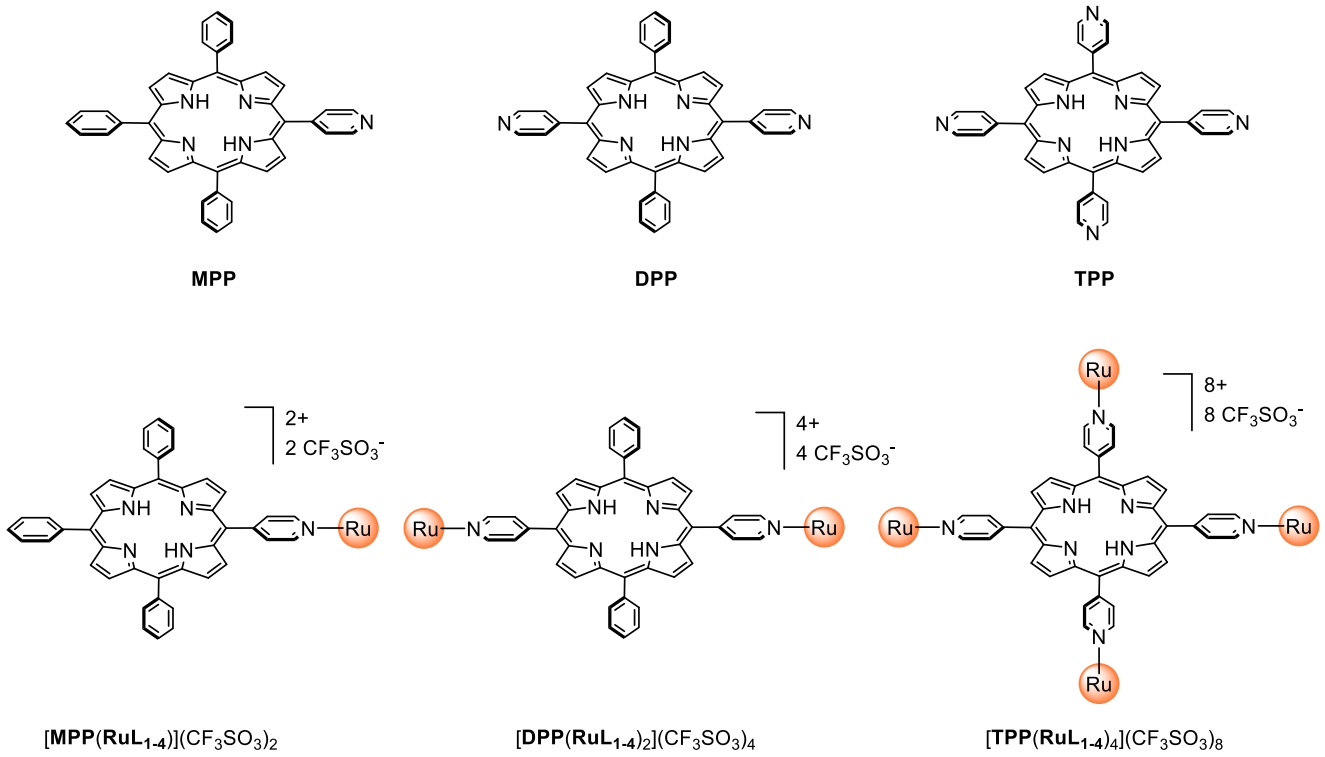

Figure 2. Molecular structures of the pyridyl porphyrins (**MPP**, **DPP**, and **TPP**) and the corresponding mono-, di- and tetra-substituted arene Ru-porphyrin-based complexes [MPP(**RuL**$_{1\text{-}4}$)](CF$_3$SO$_3$)$_2$, [**DPP**(**RuL**$_{1\text{-}4}$)$_2$](CF$_3$SO$_3$)$_4$, and [**TPP**(**RuL**$_{1\text{-}4}$)$_4$](CF$_3$SO$_3$)$_8$, the orange Ru sphere represents the RuL units at the periphery of the PS.

of O_2 near the arene Ru-porphyrin PS, an anthracenyl group has been introduced on the chelating ligand: Anthracenes being prone to react with oxygen, to form endoperoxides.[37,38] This addition of O_2 to anthracene is reversible, and can be exploited in biological applications to increase oxygen concentration at specific sites.[39]

Herein, we report the synthesis and characterization of four anthracenyl-functionalized hydrazinyl–thiazolo derivatives, their coordination to arene Ru-complexes, and the further coordination of the chelate-complexes at the periphery of three pyridyl-functionalized porphyrin-based PS. The organic hydrazinyl–thiazolo and pyridyl–porphyrin ligands, the corresponding (*p*-cymene)ruthenium complexes, and the 12 hybrid PS systems have been tested as PDT agents on the CRC cell line HCT116. The cytotoxicity of all compounds was evaluated in the dark, as well as under blue (420 nm, 20 J/cm^2), green (527 nm, 72 J/cm^2), and red (630 nm, 71 J/cm^2) light.

2. Results and Discussion

The anthracenyl–hydrazinyl–thiazole derivatives were synthesized in two steps following an established procedure (Scheme S1).[28] First, the formation of (*E*)-2-(anthracen-9-ylmethylene) hydrazine-1-carbothioamide, followed by a cyclization step with 4 different α-halocarbonyl derivatives, providing 4 anthracene-hydrazinyl-thiazole pro-ligands (**L**$_1$-**L**$_4$). Then, these molecules were coordinated to a (*p*-cymene)ruthenium unit, by reacting 0.5 equivalent of [Ru(*p*-cymene)Cl$_2$]$_2$ with 1 equivalent of **L**$_1$-**L**$_4$ in methanol (Scheme 1). All complexes were isolated as their chloride salts in excellent yield, and they have been fully characterized by ^{1}H NMR, ^{13}C NMR, UV–vis and infrared spectroscopies, as well as by mass spectrometry (see Supporting Information). The [Ru(*p*-cymene)(η^2-**L**)Cl]Cl (abbreviated [**RuL**$_{1\text{-}4}$Cl]Cl) chiral-at-metal complexes were isolated and analyzed as racemic mixtures.

Upon complexation, differences in the ^{1}H NMR spectra of **L**$_1$-**L**$_4$ with those of [Ru(*p*-cymene)(η^2-**L**)Cl]Cl confirm the coordination of **L** to Ru by two nitrogen atoms (Figures S1–S21). A downfield shift of more than 1 ppm is observed for the N—H and C—H protons of the hydrazinyl group, while the methyl group of the thiazole ring (R$_1$ in **L**$_1$-**L**$_3$) is also downfield shifted, but to a lesser extent. The complexation is further confirmed by the diastereotopic nature of the *p*-cymene protons, appearing as four doublets between 5 and 6 ppm. The coordination of **L**$_1$-**L**$_4$ to Ru is also supported by the ^{13}C NMR and infrared spectra, where changes can be observed, especially for the hydrazinyl moiety. Finally, ESI-MS in positive mode shows for all complexes the expected monocationic peak, which correspond to [Ru(*p*-cymene)**L**Cl]$^+$ after the loss of the chloride counter anion (Figures S57–S65).

Coordination of **RuL**$_{1\text{-}4}$ (**Ru** = Ru(*p*-cymene)) to three pyridyl-functionalized PS, 5-pyridyl-10,15,20-triphenylporphyrin (**MPP**), 5,15-dipyridyl-10,20-diphenylporphyrin (**DPP**), and 5,10,15,20-tetrapyridylporphyrin (**TPP**), was also performed in methanol, by a standard synthetic strategy (Scheme 2).[12] This strategy involves addition of silver triflate to extract the chlorides, followed by the addition of the pyridyl-functionalized PS (**DPP**, **MPP**, **TPP**) in an appropriate stoichiometric amount to ensure

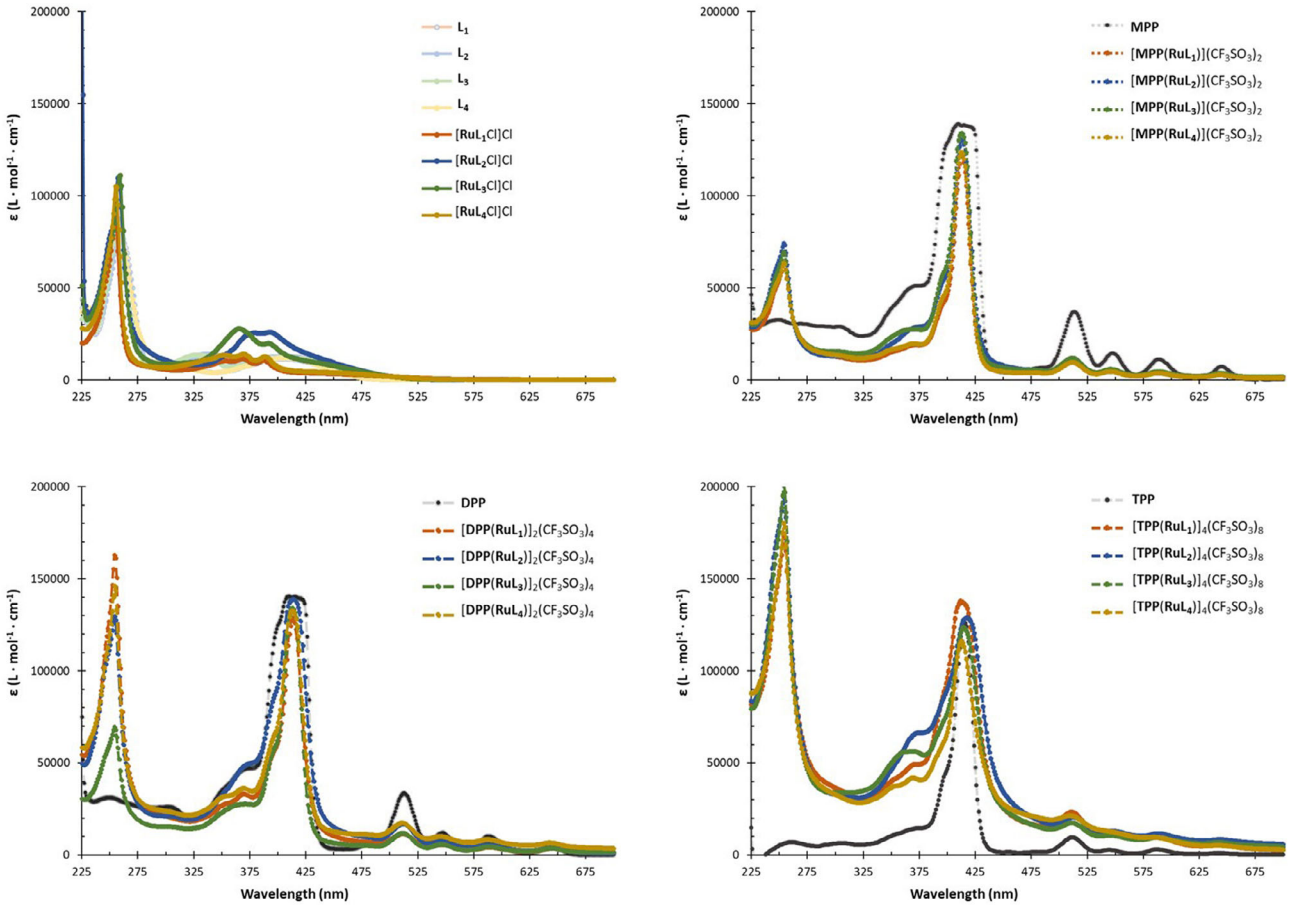

Figure 3. UV-visible spectra (1.0 x 10^{-5} M concentration) of the ligands (**L_1-L_4**), the PS (**MPP**, **DPP**, **TPP**), the [**RuL_{1-4}**Cl]Cl complexes, and the corresponding mono-, di- and tetra-substituted arene Ru-porphyrin-based complexes [**MPP**(**RuL_{1-4}**)]$(CF_3SO_3)_2$, [**DPP**(**RuL_{1-4}**)$_2$]$(CF_3SO_3)_4$, and [**TPP**(**RuL_{1-4}**)$_4$]$(CF_3SO_3)_8$.

coordination of the *N*-pyridyl atoms to Ru-centers. Then, all complexes [**MPP**(**RuL_{1-4}**)]$^{2+}$, [**DPP**(**RuL_{1-4}**)$_2$]$^{4+}$, and [**TPP**(**RuL_{1-4}**)$_4$]$^{8+}$ were isolated by filtration, after precipitation of the triflate salts upon addition of diethyl ether to the methanol solution. A schematic representation of the molecular structure of the mono-pyridyl-porphyrin (**MPP**), di-pyridyl-porphyrin (**DPP**), and tetra-pyridyl-porphyrin (**TPP**) derivatives are presented in Figure 2, together with their corresponding codenames.

Even more than the monocationic [**RuL_{1-4}**Cl]Cl complexes, the porphyrin derivatives show complexed ^{1}H NMR spectra. In addition to the diastereotopic nature of the **RuL** units, which reduces the symmetry of the functionalized PS, the pyridyl and phenyl groups of the porphyrin have limited rotational freedom, thus increasing the broadening of signals (Figures S22–S45). Nevertheless, typical signals such as the central NH porphyrin protons at ≈ −3.0 ppm, the four doublets of the aromatic *p*-cymene protons between 5 and 6 ppm, and the hydrazinyl NH proton over 11 ppm, are observed, in accordance with the expected structures (Figure 2). Moreover, ^{1}H DOSY (diffusion ordered spectroscopy) spectra show an alignment of signals, confirming the presence of only one large molecule in solution (Figures S46–S56). The ESI-MS of these large systems shows in multiple occasions the expected mass after the loss of triflate anions (Figures S66–S77).

The UV-visible spectra of the ligands and the different complexes are presented in Figure 3. The anthracenyl-functionalized hydrazinyl-thiazolo pro-ligands (**L_1-L_4**) have maxima associated to π–π^* transitions (≈ 260 nm), while the [**RuL_{1-4}**Cl]Cl complexes show additional MLCT (metal–ligand charge transfer) bands in the visible region of the spectra. On the other hand, all porphyrin-based complexes are dominated by the absorption bands of the porphyrin (**MPP**, **DPP**, **TPP**), showing an intense Soret band at 420 nm, and the typical Q bands between 475 and 675 nm.[40] The addition of **RuL** at the periphery of the PS doesn't affect the photo-physical behavior of the porphyrin core. On the other hand, the water solubility of the porphyrin-based Ru-complexes increases significantly with the number of **RuL** units, thus modifying the lipophilicity/hydrophilicity of the PS, an important factor in drug design optimization.[41]

The antiproliferative activity of the pro-ligands (**L_1-L_4**), the PS (**MPP**, **DPP**, **TPP**), the monocationic complexes [**RuL_{1-4}**Cl]Cl, as well as the 12 porphyrin-based arene Ru-systems [**MPP**(**RuL_{1-4}**)]$(CF_3SO_3)_2$, [**DPP**(**RuL_{1-4}**)$_2$]$(CF_3SO_3)_4$ and [**TPP**(**RuL_{1-4}**)$_4$]$(CF_3SO_3)_8$ have been evaluated on the CRC cell line HCT116 (see Table 1). In addition to dark toxicities, phototoxicities of the porphyrin-containing complexes [**MPP**(**RuL_{1-4}**)]$^{2+}$, [**DPP**(**RuL_{1-4}**)$_2$]$^{4+}$, and [**TPP**(**RuL_{1-4}**)$_4$]$^{8+}$, together with **MPP**, **DPP**

Table 1. IC_{50} values (nM) of pro-ligands (L_1-L_4), mononuclear arene Ru-complexes [**RuL**Cl]Cl, PS (**MPP**, **DPP**, and **TPP**), and the corresponding porphyrin-based complexes [**MPP**(**RuL**$_{1\text{-}4}$)]$(CF_3SO_3)_2$, [**DPP**(**RuL**$_{1\text{-}4}$)$_2$]$(CF_3SO_3)_4$, and [**TPP**(**RuL**$_{1\text{-}4}$)$_4$]$(CF_3SO_3)_8$ on HCT116 cancer cells after 24 h exposure, in the dark and under light (blue, green, and red).

Compound	Dark	Blue (20 J/cm^2)	Green (72 J/cm^2)	Red (71 J/cm^2)
L_1	41740 ± 10 000			
L_2	44750 ± 10 000			
L_3	36730 ± 10 000			
L_4	39880 ± 10 000			
[**RuL**$_1$Cl]Cl	7410 ± 2500	3970 ± 400		
[**RuL**$_2$Cl]Cl	7260 ± 2500	1900 ± 180		
[**RuL**$_3$Cl]Cl	4920 ± 2000	380 ± 240		
[**RuL**$_4$Cl]Cl	5200 ± 2000	5130 ± 440		
MPP	> 12 000	> 10 000	> 10 000	> 12 000
[**MPP**(**RuL**$_1$)]$(CF_3SO_3)_2$	7803 ± 297	613 ± 43	5279 ± 133	6741 ± 490
[**MPP**(**RuL**$_2$)]$(CF_3SO_3)_2$	6098 ± 513	443 ± 62	3634 ± 192	6001 ± 364
[**MPP**(**RuL**$_3$)]$(CF_3SO_3)_2$	5623 ± 318	575 ± 27	3485 ± 205	5548 ± 408
[**MPP**(**RuL**$_4$)]$(CF_3SO_3)_2$	5813 ± 216	600 ± 41	3539 ± 227	5753 ± 247
DPP	> 6000	> 6000	> 6000	> 6000
[**DPP**(**RuL**$_1$)$_2$]$(CF_3SO_3)_4$	5322 ± 116	15.5 ± 2.75	136 ± 1.08	810 ± 16
[**DPP**(**RuL**$_2$)$_2$]$(CF_3SO_3)_4$	4828 ± 321	2.39 ± 0.5	40.3 ± 1.66	250 ± 6
[**DPP**(**RuL**$_3$)$_2$]$(CF_3SO_3)_4$	3706 ± 136	2.62 ± 0.42	51.0 ± 1.70	256 ± 37
[**DPP**(**RuL**$_4$)$_2$]$(CF_3SO_3)_4$	5643 ± 278	7.37 ± 1.33	43.7 ± 3.0	354 ± 157
TPP	> 5000	> 5000	> 5000	> 5000
[**TPP**(**RuL**$_1$)$_4$]$(CF_3SO_3)_8$	3062 ± 59	11 ± 0.6	48.3 ± 1.67	223 ± 19
[**TPP**(**RuL**$_2$)$_4$]$(CF_3SO_3)_8$	2010 ± 54	9 ± 0.5	42 ± 1.4	292 ± 25
[**TPP**(**RuL**$_3$)$_4$]$(CF_3SO_3)_8$	1761 ± 37	16 ± 1	46 ± 1.8	580 ± 10
[**TPP**(**RuL**$_4$)$_4$]$(CF_3SO_3)_8$	2231 ± 58	20.3 ± 1.95	49 ± 0.8	578 ± 71

and **TPP**, were determined under blue (420 nm, 20 J/cm^2), green (527 nm, 72 J/cm^2), and red (630 nm, 71 J/cm^2) light irradiation, and the proliferative activity evaluated 24 h after light exposure.

The cytotoxicity in the dark of the various compounds is clearly linked to the presence of the **RuL** units (see Table 1, 2nd column). The anthracenyl–hydrazinyl–thiazole ligands (**L**$_{1\text{-}4}$) show modest activity in the dark with IC_{50} values at ≈ 40 µM, being by far the less cytotoxic compounds. On the other hand, the **RuL** derivatives show IC_{50} values slightly below 10 µM, with the most cytotoxic being the [**TPP**(**RuL**)$_4$]$^{4+}$ derivatives at around 2 µM, which contains 4 units of **RuL**. Such IC_{50} values are not surprising, as most arene Ru-complexes show activity in the µM range,[42–44] and these metal-based derivatives are no exception. However, the **RuL** units are not only providing a degree a toxicity, they also increase significantly the water solubility of the PS by limiting aggregation and adding charges. Indeed, without complexation of **RuL** at the periphery of the PS, their poor solubility does not allow a precise determination of their IC_{50} values, having the tendency to aggregate.[14,15] Nevertheless, like all compounds studied, the IC_{50} values of **MPP**, **DPP**, and **TPP** remain in the µM range, and appear to be less cytotoxic than the Ru-functionalized counterpart.

Interestingly, when light is applied, the activity is quite different, and the benefit of combining **RuL** with pyridyl-porphyrin PS (**MPP**, **DPP**, and **TPP**) can be fully appreciated, as illustrated in Table 1. Alone, all PS are showing activity > 5 µM on HCT116 cancer cells, at the three wavelengths studied 420 nm (20 J/cm^2), 527 nm (72 J/cm^2) and 630 nm (71 J/cm^2), respectively. However, when multiple **RuL** units are added to the PS, two **RuL** units with **DPP** and four units with **TPP**, the phototoxicity increases significantly, reaching the low nM range, and having a wide phototoxic index (ratio between light and dark toxicities). Indeed, some IC_{50} values under blue light (420 nm) are as low as 3 nM for the dipyridyl-porphyrin derivatives [**DPP**(**RuL**$_2$)$_2$]$(CF_3SO_3)_4$ and [**DPP**(**RuL**$_3$)$_2$]$(CF_3SO_3)_4$, with a phototoxic index of about 2000. The [**DPP**(**RuL**$_2$)$_2$]$(CF_3SO_3)_4$ complex is also the most active under green light with an IC_{50} of 40 nM and a phototoxic index of 100. Even under red light irradiation, the [**DPP**(**RuL**)$_2$]$(CF_3SO_3)_4$ and [**TPP**(**RuL**)$_4$]$(CF_3SO_3)_8$ show phototoxicity in the nM range, with a good phototoxic index. However, the mono-functionalized PS [**MPP**(**RuL**)]$(CF_3SO_3)_2$ complexes, the less water soluble, show activity only in the superior nM range.

3. Conclusion

Twelve hybrid PS systems built from four easily synthesized anthracenyl-functionalized hydrazinyl-thiazolo arene ruthenium complexes and three commercially available pyridyl-functionalized porphyrin-based PS have been prepared in excellent yields. All organometallic PS show a degree of photo-

toxicity, which can be modulated by the presence of the arene ruthenium units at the periphery of the PS. In the dark, the toxicity remains in the μM range for all complexes, while under light, when two or four arene ruthenium units are surrounding the polypyridyl–porphyrin PS (**DPP**, **TPP**) the phototoxicity shifts in the nM range, with tremendous phototoxic indexes. The most active compounds being those with two organometallic complexes per PS. Therefore, in view of these results, design optimization strategies can be deployed, by modulating the nature and number of the hydrazinyl-thiazolo arene ruthenium units, as well as the polypyridyl-functionalized PS (chlorin, bacteriochlorin, phthalocyanines, with 2, 3 or 4 coordinating groups), ultimately, being an ideal platform for a modular synthetic approach.[45,46]

Supporting Information

Experimental details and spectral data for all new compounds are available in the supporting information

Acknowledgments

The authors thank the University of Neuchatel for financial support.

Open access publishing facilitated by Universite de Neuchatel, as part of the Wiley - Universite de Neuchatel agreement via the Consortium Of Swiss Academic Libraries.

Conflict of Interests

The authors declare no conflict of interest.

Data Availability Statement

The data that support the findings of this study are available from the corresponding author upon reasonable request.

Keywords: Anthracene · Arene ruthenium · HCT116 colon cancer cells · Photodynamic therapy · Photosensitizer

[1] P. Charlesworth, T. G. Truscott, R. C. Brooks, B. C. Wilson, *J. Photochem. Photobiol. B: Biol.* **1994**, *26*, 277–282.
[2] M. J. Abrams, *Platinums Metal Rev.* **1995**, *39*, 14–18.
[3] M. J. Clarke, *Coord. Chem. Rev.* **2003**, *236*, 209–233.
[4] L. Zeng, P. Gupta, Y. Chen, E. Wang, L. Ji, H. Chao, Z.-S. Chen, *Chem. Soc. Rev.* **2017**, *46*, 57715804.
[5] F. Li, G. Collins, F. R. Keene, *Chem. Soc. Rev.* **2015**, *44*, 25292542.
[6] D. E. J. G. J. Dolmans, D. Fukumura, R. K. Jain, *Nat. Rev. Cancer* **2003**, *3*, 380387.
[7] B. Jing, M. Zhang, T. Shen, *Org. Lett.* **2003**, *5*, 3709–3711.
[8] J. Zhou, J. Liu, Y. Feng, S. Wei, X. Gu, X. Wang, B. Zhang, *Bioorg. Med. Chem. Lett.* **2005**, *15*, 3067–3070.
[9] H. Shi, R. C. Marchi, P. J. Sadler, *Angew. Chem. Int. Ed.* **2025**, *64*, e202423335.
[10] M. A. Munegowda, A. Manalac, M. Weersink, S. A. McFarland, L. Lilge, *Coord. Chem. Rev.* **2022**, *470*, 214712.
[11] K. Davia, D. King, Y. Hong, S. Swavey, *Inorg. Chem. Commun.* **2008**, *11*, 584–586.
[12] F. Schmitt, P. Govindaswamy, G. Süss-Fink, W. H. Ang, P. J. Dyson, L. Juillerat-Jeanneret, B. Therrien, *J. Med. Chem.* **2008**, *51*, 18111816.
[13] T. Gianferrara, A. Bergamo, I. Bratsos, B. Milani, C. Spagnul, G. Sava, E. Alessio, *J. Med. Chem.* **2010**, *53*, 46784690.
[14] J. H. Correira, J. A. Rodrigues, S. Pimenta, T. Dong, Z. Yang, *Pharmaceutics* **2021**, *13*, 1332.
[15] J. Dai, X. Wu, S. Ding, X. Lou, F. Xia, S. Wang, Y. Hong, *J. Med. Chem.* **2020**, *63*, 19962012.
[16] F. Bächle, N. Siemens, T. Ziegler, *Eur. J. Org. Chem.* **2019**, *2019*, 7089.
[17] G. Süss-Fink, *J. Organomet. Chem.* **2014**, *751*, 2.
[18] B. Therrien, *Coord. Chem. Rev.* **2009**, *253*, 493.
[19] Y. K. Yan, M. Melchart, A. Habtemariam, P. J. Sadler, *Chem. Commun.* **2005**, *41*, 4764.
[20] R. Kushwaha, S. Banerjee, *ChemBioChem* **2025**, *26*, e202400931.
[21] P. Priya Arun, R. Raj Patel, S. Kumar Singh, K. Parmar, M. Singh, *J. Organomet. Chem.* **2025**, *1035*, 123682.
[22] R. Mondal, M. Kunhumon Noushija, S. P. Banu, N. Pandurangan, S. Shanmugaraju, *Inorg. Chim. Acta* **2024**, *569*, 122156.
[23] Z. Janbeih, M. Gallardo-Villagrán, B. Therrien, M. Diab-Assaf, B. Liagre, L. Benov, *Inorganics* **2024**, *12*, 86.
[24] M. Gallardo-Villagrán, L. Paulus, Y. Champavier, D. Y. Leger, B. Therrien, B. Liagre, *J. Porphyrins Phthalocyanines* **2022**, *26*, 535541.
[25] M. Patra, T. Joshi, V. Pierroz, K. Ingram, M. Kaiser, S. Ferrari, B. Spingler, J. Keiser, G. Gasser, *Chem. Eur. J.* **2013**, *19*, 14768.
[26] Y. Ma, Z. Zhang, F. Sun, P. Mesdom, X. Ji, P. Burckel, G. Gasser, M.-H. Li, *Biomacromol* **2023**, *24*, 59405950.
[27] U. Salar, K. M. Khan, S. Chigurupati, M. Taha, A. Wadood, S. Vijayabalan, M. Ghufran, S. Perveen, *Sci. Rep.* **2017**, *7*, 16980.
[28] A. Grozav, L. I. Găină, V. Pileczki, O. Crisan, L. Silaghi-Dumitrescu, B. Therrien, V. Zaharia, I. Berindan-Neagoe, *Int. J. Mol. Sci.* **2014**, *15*, 22059-22072.
[29] C. Soh, L. Shadap, M. R. Kollipara, J. L. Tyagi, K. M. Poluri, Y. Mozharivskyj, E. K. Rymmai, *J. Organomet. Chem.* **2023**, *984*, 122559.
[30] A. Grozav, T. Cheminel, A. Jurj, O. Zanoaga, L. Raduly, C. Braicu, I. Berindan-Neagoe, O. Crisan, L. Gaina, B. Therrien, *Inorganics* **2024**, *12*, 287.
[31] A. Grozav, O. Balacescu, L. Balacescu, T. Cheminel, I. Berindan-Neagoe, B. Therrien, *J. Med. Chem.* **2015**, *58*, 84758490.
[32] S. Dey, A. Das, F. Hossain, *Chem. Select* **2020**, *5*, 15153.
[33] I. Mármol, C. Sánchez-de-Diego, A. Pradilla Dieste, E. Cerrada, M. J. Rodriguez Yoldi, *Int. J. Mol. Sci.* **2017**, *18*, 197.
[34] K. Simon, *Clin. Interv. Aging* **2016**, *11*, 967.
[35] R. N. Schwartz, C. D. Blanke, L. J. Pesko, *J. Manag. Care Pharm.* **2004**, *10*, S2.
[36] J. A. Rodrigues, J. H. Correia, *Int. J. Mol. Sci.* **2023**, *24*, 12204.
[37] E. L. Clennan, *Photochem. Photobiol.* **2023**, *99*, 204–220.
[38] R. Palabindela, P. Myadaravenia, D. Banothu, R. Korra, H. Mekala, M. Kasula, *Orient. J. Chem.* **2022**, *38*, 137–143.
[39] C. Pierlot, V. Rataj, J.-M. Aubry in, *Singlet Oxygen: Applications in Biosciences and Nanosciences*, (Eds: S. Nonell, C. Flors), The Royal Society of Chemistry, Cambridge, UK, **2016**, *1*, 47–73.
[40] H. Imahori, T. Umeyama, S. Ito, *Acc. Chem. Res.* **2009**, *42*, 1809–1818.
[41] S. A. Putri, R. Maharani, I. P. Maksum, T. J. Siahaan, *Drug Des. Devel. Ther.* **2025**, *19*, 645–670.
[42] O. A. Lenis Rojas, S. Cordeiro, P. V. Baptista, A. R. Fernandes, *J. Inorg. Biochem.* **2023**, *245*, 112255.
[43] P. Chellan, P. J. Sadler, *Chem. - Eur. J.* **2020**, *26*, 8676–8688.
[44] B. S. Murray, M. V. Babak, C. G. Hartinger, P. J. Dyson, *Coord. Chem. Rev.* **2016**, *306*, 86–114.
[45] A. M. Korolchuk, V. A. Zolottsev, A. Y. Misharin, *Top. Curr. Chem.* **2023**, *381*, 10.
[46] S. Kumari, A. V. Carmona, A. K. Tiwari, P. C. Trippier, *J. Med. Chem.* **2020**, *63*, 12290–12358.

Manuscript received: September 12, 2025